



Contents lists available at ScienceDirect

North American Spine Society Journal (NASSJ)

journal homepage: www.elsevier.com/locate/xnsj

Clinical Studies

The technique of using three-dimensional and multiplanar reformatted computed tomography for preoperative planning in pediatric craniovertebral anomalies

Kshitij Chaudhary^{a,*}, Arjun Dhawale^{a,b}, Avi Shah^b, Abhay Nene^b^a Department of Orthopaedics, Sir HN Reliance Foundation Hospital, Raja Ram Mohan Roy Road, Mumbai, Maharashtra, India^b Department of Pediatric Orthopaedics, Bai Jerbai Wadia Hospital for Children, Acharya Dhonde Marg, Mumbai, Maharashtra, India

ARTICLE INFO

Keywords:

Pediatric
Craniovertebral
Atlantoaxial instability
Preoperative planning
Multiplanar reconstruction

ABSTRACT

Background: Computed tomography (CT) images provided by the radiology department may be inadequate for planning screws for rigid craniovertebral junction (CVJ) instrumentation. Although many recommend using multiplanar reconstruction (MPR) in line with screw trajectories, this is not always available to all surgeons. The current study aims to present a step-by-step workflow for preoperative planning for pediatric CVJ anomalies.

Methods: Twenty-five consecutive children (<12 years) were operated for atlantoaxial instability between 2014 and 2019. Preoperative CT angiograms were transferred to an open-source software called Horos™. The surgeon manipulated images in this viewing software to determine an idealized path of screws. Three-dimensional volume rendering of the pathoanatomy was generated, and anomalies were noted. The surgeon compared the anatomical data obtained using Horos™ with that from the original imaging platform and graded it as; Grade A (substantial new information), Grade B (confirmatory with improved visualization and understanding), Grade C (no added information). The surgeon then executed the surgical plan determined using Horos™.

Results: Surgeries performed were occipitocervical ($n = 18$, 72%) and atlantoaxial fixation ($n = 7$, 28%) at a mean age of 7.2 years, with 72% of etiologies being congenital or dysplasias. In 18 (72%) patients, the surgeon noted substantial new information (Grade A) about CVJ anomalies on Horos™ compared to original imaging platform. Concerning planning for fixation anchors, the surgeon graded A in all patients (100%). In 4 (16%) patients, the surgery could not be executed precisely as planned. There were three (12%) complications; VA injury ($n = 1$), neurological worsening ($n = 1$), and loss of fixation ($n = 1$).

Conclusion: In our experience, surgeon-directed imaging manipulation gives more anatomical information compared to studying original imaging planes and should be incorporated in the surgeon's preoperative workup. When image reformatting options are limited, open-source software like Horos™ may offer advantages.

Introduction

Many studies have shown that rigid instrumentation of pediatric craniovertebral junction (CVJ) anomalies has a lower complication and higher fusion rate than wiring constructs [1]. However, rigid instrumentation for CVJ anomalies in children can be challenging [2,3]. Preoperative planning on computed tomography (CT) is essential to ensure precise surgical execution [2,4].

Usually, the CT scan as assessed on the hospital's Picture Archive and Communication System (PACS) is in the form of two-dimensional DICOM (Digital Imaging and Communications in Medicine) images in the three standard orthogonal planes (axial, coronal, and sagittal). How-

ever, the slice orientation of such images may not be in line with the proposed screw trajectory and may be inadequate for planning [5–8]. Therefore, many experts recommend a multiplanar reformatting (MPR) of the images in-line with the screw's proposed trajectory to determine whether the bone will accept the planned screw [7–9].

Many PACS end-user interfaces do not have MPR capabilities required for manipulating the DICOM images. In these situations, surgeons either have to use the workstations in the radiology department to reformat DICOM images in non-orthogonal planes or use PACS that specifically allow for MPR [8]. Although preoperative planning on radiology workstations is better than scrolling through PACS images, the time that the radiology department can spare their workstation for this purpose may be limited.

* Corresponding author.

E-mail address: dr_kshitij.chaudhary@hindujahospital.com (K. Chaudhary).<https://doi.org/10.1016/j.xnsj.2021.100073>

Received 9 May 2021; Received in revised form 1 July 2021; Accepted 3 July 2021

Available online 14 July 2021

2666-5484/© 2021 The Authors. Published by Elsevier Ltd on behalf of North American Spine Society. This is an open access article under the CC BY-NC-ND license (<http://creativecommons.org/licenses/by-nc-nd/4.0/>)

The development of open-source software has added radiology workstation capabilities to personal computers. Horos™ is one such open-source software that is distributed free of charge under the Lesser General Public License at Horosproject.org and sponsored by Nimble Co LLC d/b/a Purview in Annapolis, MD, USA. Although Horos™ itself is not FDA approved, it was developed on the OsiriX™ platform (Pixmeo Company, Geneva, Switzerland); a commercial FDA approved software used by radiology departments worldwide.

Open software like Horos™ may be useful for surgeons working in hospitals which do not have PACS with MPR functionality. To our knowledge, there is only one small clinical study of five adult patients demonstrating the usefulness of OsiriX™ in planning C2 pedicle screws [7]. We have applied this method of preoperative planning to pediatric CVJ patients and have used it for planning idealized trajectory for the C2 laminar screw and transarticular screw, in addition to the C2 pedicle screw.

In the current study, we aim to present a step-by-step workflow for planning screw trajectory and assessment of three-dimensional (3D) pathoanatomy of pediatric CVJ anomalies such that surgeons can do these steps themselves using Horos™ software. We evaluate whether this method of preoperative planning can provide additional anatomical information compared to conventional PACS. We also report the clinico-radiological outcomes of these children.

Methods

Study cohort

After obtaining ethics committee approval for the current study, 25 consecutive children younger than 12 years with atlantoaxial instability, operated by two fellowship-trained spine surgeons between January 2014 and December 2019 were identified. Demographic data, primary diagnosis, presenting symptoms, and preoperative neurology (motor function scoring system of the Japanese Orthopaedic Association (JOA) were collected [10].

Imaging data

All patients had preoperative cervical radiographs, magnetic resonance imaging (MRI), and CT scans with vertebral artery (VA) angiogram. The CT images, provided by the radiology department, were available on the hospital PACS and were labeled as PACS CT. These contained orthogonally reconstructed images in axial, coronal, and sagittal planes of the cervical spine and 3D volume-rendered 3D images of the CVJ in fixed projections. The operating surgeon studied the PACS CT data and developed a tentative preoperative plan.

Horos software was downloaded on the surgeon's laptop (Apple MacBook) from <https://horosproject.org>. Anonymized CT DICOM data was exported to a CD-ROM from PACS. The CD-ROM contents were transferred to Horos™ software. The surgeon then manipulated the DICOM images to assess screw feasibility and determined the idealized path of screw anchors in the following four steps (Video Supplement 1):

Step 1: Multiplanar reconstruction (MPR) was used to create true axial, coronal, and sagittal images of the C2 vertebra (Figs. 1d–f, 2d–f, 3d–f)

Step 2: The axes were manipulated to create para-sagittal (Figs. 1g, 2g, 3g) and para-axial images (Figs. 1h, 2h, 3h) showing the longitudinal axis of the screw trajectory [7]. The para-coronal plane (Figs. 1i, 2i, 3i) that is orthogonal to these para-sagittal and para-axial images represents the true cross-section of the screw path. The smallest diameter at the narrowest cross-section on the para-coronal images was measured to determine screw feasibility. The smallest diameter screw available was 3 mm, except for transarticular screw (TAS), which was available in 2.7 mm. Therefore, the screw path was considered feasible if the diameter was >3.2 mm for TAS and >3.5 mm for the other screws.

Step 3: The long axis of the screw trajectory in the para-axial plane (Figs. 1h, 2h, 3h) was used to determine the entry point of the screw, which was marked with a fiducial marker.

Step 4: 3D volume rendering of the pathoanatomy was then created (Figs. 1j, 2j, 3j). The 3D image was cropped using the “scissor” tool such that only the desired anatomy was visible. The fiducial markers were visualized on the bone's surface and were used intraoperatively to decide the entry point of the screw. Morphological anomalies of the occiput, C1, C2, and subaxial cervical vertebrae were systematically noted by manipulating this 3D image on the computer in any projection desired.

Vertebral artery (VA) anomalies (course, caliber, and abnormal branches) were looked for in the V₃1 (intraosseous part of VA), V₃2 (from C2 transverse foramen to C1 transverse foramen), and V₃3 (from C1 transverse foramen to its entry into the dural sac) segment of the VA [11]. In patients with assimilated atlas, the VA course was classified into three types, according to the classification proposed by Wang et al. [12]. A high riding vertebral artery (HRVA) was identified on MPR images if the in-line trajectory of TAS or C2PS was interrupted by the vertebral artery cave. A dominant vertebral artery was defined if the lumen on one side was twice that of the other (ratio of >2.0) [13]. After planning, the reconstructed DICOM images were saved and were accessed on the surgeon's laptop in the operating room.

Grading

Two aspects of the anatomical information were graded; (1) pathoanatomy and (2) feasibility of fixation anchors. For each aspect, the operating surgeon graded the preoperative information obtained by using Horos™ against the information received from the PACS CT using a grading system that has been previously used by Newton et al. [14] in their publication comparing the usefulness of multiplanar and 3D CT reconstructions versus conventional 2D CT scan for congenital scoliosis.

Grade A (substantial new information obtained)

Grade B (confirmatory with improved visualization and understanding)

Grade C (no added information obtained)

Surgical plan

All patients underwent occipitocervical (OC) or atlantoaxial fusion by the posterior approach. On traction and under general anesthesia and muscle relaxation, patients were classified as anatomically reducible (complete realignment), partially reducible (partial realignment), or irreducible (no change in alignment). OC fusion was chosen over atlantoaxial fusion in patients with atlas assimilation or in those where C1 lateral mass screw (C1LMS) was not feasible.

Occipital anchors were always in the occipital keel in the midline. The choice of C2 fixation in OC fusion was C2 pedicle screw (C2PS), C2 laminar screw (C2LAM), or C2 pars screw (C2PaS), in decreasing order of preference. C2LAM was chosen over the C2PS in most patients with C2-3 congenital fusion, even if the C2PS trajectory was feasible. For atlantoaxial fusion, the TAS (transarticular screw) was the first choice in patients who had favorable anatomy and anatomical reduction. If TAS was not feasible, then a C1-C2 fixation was chosen.

Any deviations or surprises inconsistent with preoperative planning were recorded. Complications were reviewed. Postoperative neurology was documented at each follow-up. Fusion was assessed on a CT scan done between 3 and 6 months postoperatively, and successful fusion was defined as continuity of bone trabeculae either across the posterior elements or across the atlantoaxial joints.

Results

Patients studied

The demographics of this patient cohort is summarized in Table 1. The mean age was 7.20 years (range: 26 months - 12 years). There

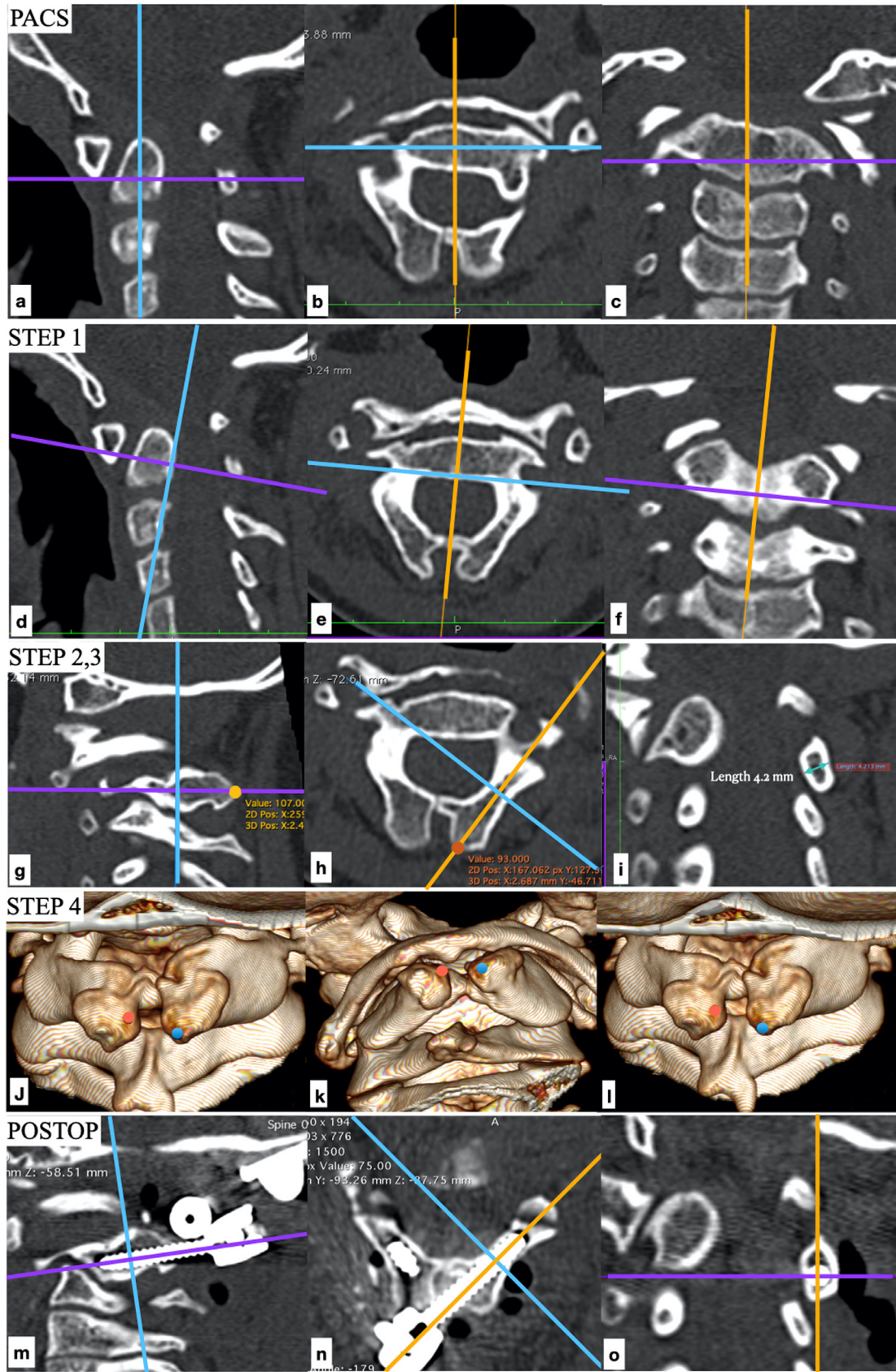


Fig. 1. Planning of C2 laminar screw for Case 25. Steps described in the manuscript and the video supplement 1.

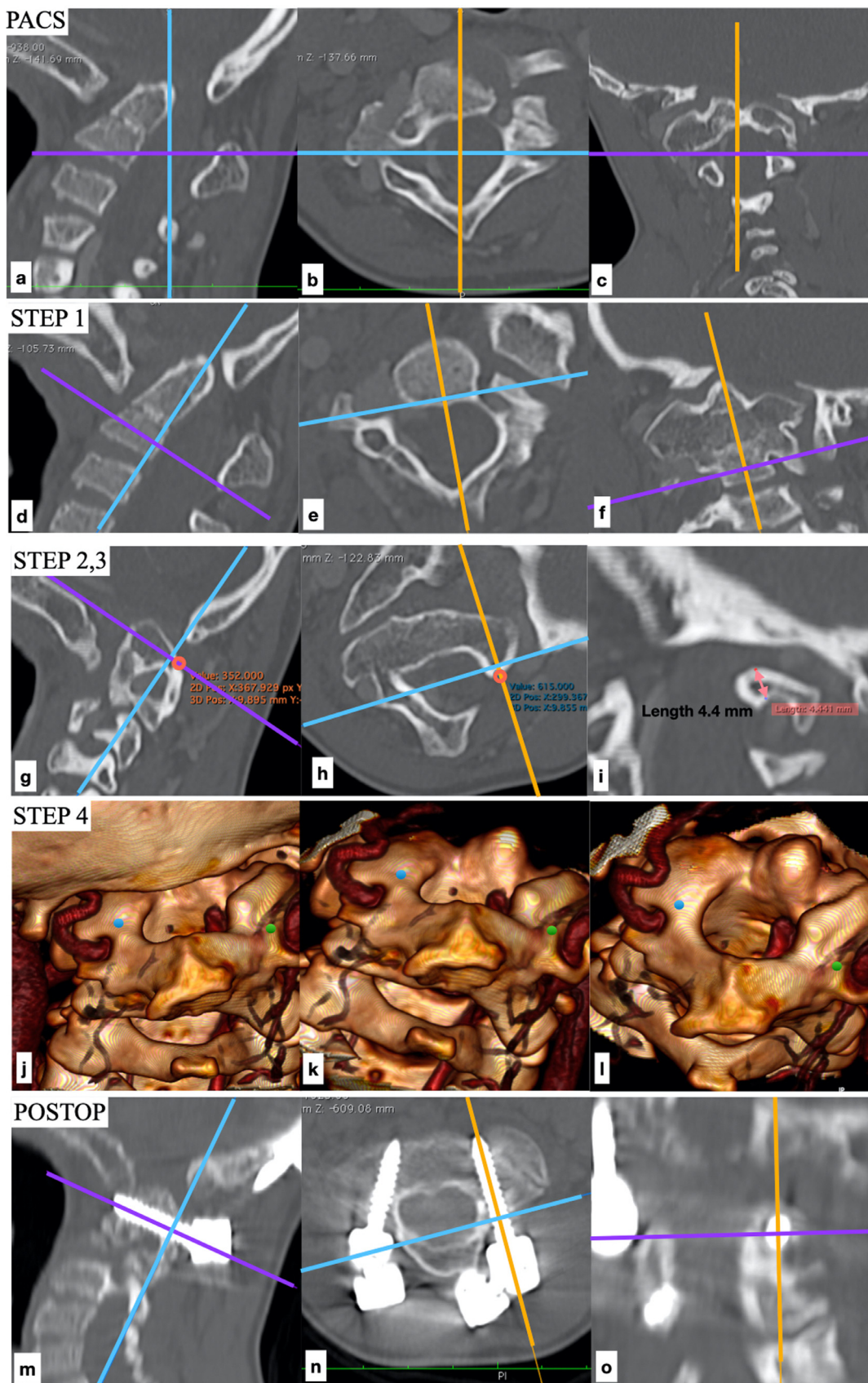


Fig. 2. Planning of C2 pedicle screw for Case 15. Steps described in the manuscript and the video supplement 1.

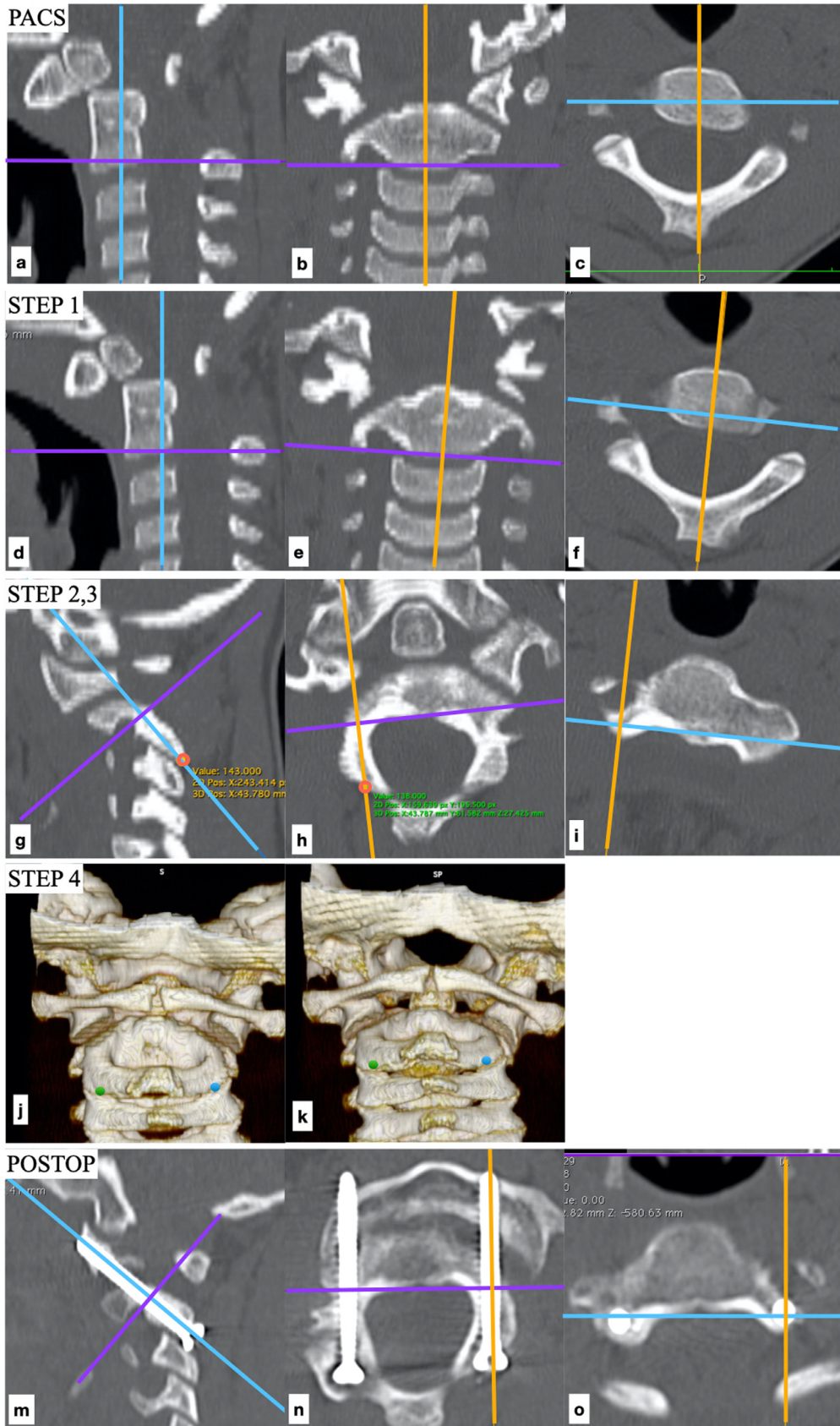


Fig. 3. Planning of transarticular screw for Case 9. Steps described in the manuscript and the video supplement 1.

Table 1
Demographics, treatment, and outcomes of 25 patients.

Demographics	
Age	7.2y (26 months -12 years)
M:F	13:12
Etiology	
Congenital	11 (44%)
Skeletal Dysplasia	7 (28%)
Os Odontoideum	5 (20%)
Down Syndrome	2 (8%)
Clinical Presentation	
Myelopathy	25 (100%)
mJOA (UE)	2.3 (1–5)
mJOA (LE)	2.4 (2–6)
Torticollis	1 (4%)
Neck pain	2 (8%)
History of trauma	3 (12%)
Reducibility	
Complete reducibility	17 (68%)
Partial reducibility	8 (32%)
Surgery	
Occipitocervical fusion	18 (72%)
Atlantoaxial fusion	7 (28%)
Foramen magnum decompression	10 (40%)
C1 laminectomy	10 (40%)
Fixation anchors	
C2 laminar screws	20
C2 pedicle screws	10
Transarticular screws	10
Laminar hook	6
C1 lateral mass screw	5
C2 pars screw	4
Subaxial lateral mass screw	4
Mersilene tape	2
C3 pedicle screw	1
C3 laminar screw	1
Clinical Outcomes	
Postoperative mJOA UE	4.3 (0–5)
Postoperative mJOA LE	5.8 (1–7)
Radiological Outcome	
Fusion	25 (100%)
Screw violation of vertebral artery cave	3 (12.5%)
Partial loss of initial reduction	3 (12%)

were 13 males and 12 females. The spectrum of etiology was congenital anomalies ($n = 11$), skeletal dysplasia ($n = 7$), isolated os odontoideum ($n = 5$), and Down syndrome ($n = 2$). Among the skeletal dysplasia patients, three were diagnosed with Morquio syndrome.

All children presented with a neurological abnormality (Table 1). Average preoperative mJOA (modified Japanese Orthopaedic Association) score in upper (UE) and lower extremity (LE) was 2.3 (range 1–5) and 2.4 (range 2–6), respectively. Three children presented to the pediatrician with delayed motor milestones that led to the diagnosis. Other presentations were torticollis ($n = 1$), neck pain ($n = 2$) and neck trauma ($n = 3$).

Radiographic findings

MRI showed a hyperintense signal in the spinal cord in 13 patients (52%), out of which three patients (12%) had syringomyelia and syringobulbia. Surgeon-directed CT DICOM manipulation on Horos™ revealed the following:

Pathoanatomy (Table 2): Seven (28%) patients had basilar invagination. Five (20%) patients had atlas assimilation. Five (20%) patients had atlantal hemi-rings with splaying of the lateral masses. Anomalies of the dens were; aplasia (4), hypoplasia (7), and os (8). Ten (40%) patients had congenital C2-3 posterior element fusion, including one patient with a congenital fusion from C2 to C6. Dysplastic subaxial cervical spine was noted in five (20%) patients. One patient had bilateral C2 pars lysis (Fig. 4a). Another one had a complete absence of the C2 neural arch (Fig. 4b). Ten (40%) patients had at least one-sided high riding vertebral artery (HRVA) (Unilateral HRVA, $n = 5$; Bilateral HRVA, $n = 5$). The

course of the V₃ segment of VA in patients with atlas assimilation was Type 1 ($n = 4$), Type 2 ($n = 3$), and Type 3 ($n = 3$) [12]. Three (12%) patients had a persistent first intersegmental vertebral artery with the VA coursing underneath the C1 arch unilaterally. The VA caliber was either codominant ($n = 17$), left dominant ($n = 4$), or right dominant ($n = 4$).

Planning of screw anchors: The planning of screw anchors for individual cases is enumerated in Table 3. The overall distribution of fixation anchors in the upper cervical spine was: C2 laminar screws (20), C2 pedicle screws (10), transarticular screws (10), Laminar Hook (6), C1 lateral mass screws (5), C2 pars screw (4), subaxial cervical lateral mass screw (4), mersilene tape (2), C3 pedicle screw (1), C3 laminar screw (1). Table 4 summarizes the reasons for the unsuitability of screws in C1 and C2.

In 10 patients with congenital C2-3 fusion, 4 of the 20 sites (20%) were unsuitable for C2 laminar screws (C2LAM) as the lamina was too thin. Of the remaining 16 sites, 15 (93.7%) were used for C2LAM screws in patients with C2-3 fusion. Altered entry points (uncrossed trajectory) for C2LAM screw were noted for 13 laminae of 7 patients. 7 of the 13 laminae were successfully instrumented (Fig. 5b). Out of these seven patients, a 11-year-old (Case 25) had an incomplete midline closure of the C2 neural arch. The other six patients had underdeveloped C2 spinous process either because they had skeletal dysplasia ($n = 3$) or they were under 5-years of age ($n = 3$). All occipital anchors were in the midline occipital keel, except in one patient where the keel was not in the midline (Case 11, Fig. 5f)

Surgeon's grading of preoperative planning

Concerning pathoanatomy information (Table 2) obtained on Horos™, Grade A (substantial new information) was noted in 18 patients (72%), and Grade B (improved visualization of anatomy) was noted in 5 patients (20%). Grade C (no new information) recorded in only two patients (8%) who had no other anomaly except os odontoideum.

Concerning surgical planning for screw-based anchors (Table 3), the surgeon graded all cases as Grade A (100%), where substantial new information was obtained compared to PACS CT. Cervical screw fixation proved impossible in two dysplastic children, despite planning on Horos™ (Cases 8 and 23).

In 4 (16%) patients, the surgery could not be executed precisely as planned Horos™.

- 1 Case 2: C3 lateral mass screw cut out intraoperatively and was replaced with a hook and had an uneventful outcome.
- 2 Case 5: C1LMS was avoided after V₃1 segment VA injury. C1-C2 fusion was converted to O-C2 fusion. The patient did not have a postoperative deficit and recovered uneventfully.
- 3 Case 8: Intraoperatively, planned C2 laminar screws cut out of bone. No other suitable sites were available, and hence subaxial laminar hooks were used. However, laminae were too soft and small for the hooks, one of which migrated in the canal resulting in a neurological deficit.
- 4 Case 23: C2LAM cut out intraoperatively. As no other suitable site was available, sublaminar mersilene tapes were used, followed by prolonged postoperative rigid bracing.

Surgery

The subluxations were anatomically reducible in 17 (68%) patients, and partially reducible in 8 (32%) patients when assessed with traction under anesthesia (Table 1). Eighteen patients (72%) had OC fixation, seven had atlantoaxial fixation (28%). Of the seven, five (20%) had TAS fixation, two patients (8%) had segmental atlantoaxial fixation. Ten (40%) patients had a foramen magnum decompression, and ten (40%) had a C1 laminectomy (Table 1). Average blood loss was 164 ml (range

Table 2
Systematic description of pathoanatomy of various anomalies as detected on Horos™.

	Age	Etiology	Occiput	C1	C2	C3-C7	Vertebral Artery (VA)	Grade
Case 1	7+3y, M	Skeletal Dysplasia [†]	Basilar [#] – No anomaly Condylar [#] – No anomaly Squama [#] – No anomaly	No anomalies Facets – No anomaly	Dens – Os Neural arch – C2-3 fusion	Posterior element fusion from C2 to C6	V ₃ 1 – No anomaly V ₃ 2 – No anomaly V ₃ 3 – No anomaly Left dominant VA	A
Case 2	11+4y, F	Skeletal Dysplasia [*]	Basilar – No anomaly Condylar – Hypoplasia Squama – No anomaly	Ant. arch – bifid Post. arch – bifid LM – splayed Facets – dysplasia	Dens – aplasia Neural arch – No anomaly	Dysplasia	V ₃ 1 – Bilateral HRVA V ₃ 2 – No anomaly V ₃ 3 – No anomaly Codominant VA	A
Case 3	12y, M	Congenital Anomaly [†]	Basilar – No anomaly Condylar – Hypoplasia Squama – No anomaly	Ant. arch – assimilated Post. arch – [R] arch absent LM – [R] assimilated Facets – Vertical oriented	Dens – No anomaly Neural arch – C2-3 fusion	No anomaly below C3	V ₃ 1 – Bilateral HRVA V ₃ 2 – No anomaly V ₃ 3 – Type 1 (bilateral) Codominant VA	A
Case 4	6+4y, M	Congenital Anomaly [†]	Basilar – Platybasia Condylar – Deformed Squama – No anomaly	Complete atlas assimilation In-curling of posterior arch Facets – Vertical oriented	Dens – No anomaly Neural arch – C2-3 fusion	No anomaly below C3	V ₃ 1 – [R] HRVA; [L] No anomaly V ₃ 2 V ₃ 3 – [L] Type 2 and [R] Type 3 Right dominant VA	A
Case 5	8+4y, F	Os odontoideum	Basilar – No anomaly Condylar – No anomaly Squama – No anomaly	No anomalies Facets – No anomaly	Dens – Os Neural arch – No anomaly	No anomaly	V ₃ 1 – No anomaly V ₃ 2 – No anomaly V ₃ 3 – No anomaly Left dominant VA	B
Case 6	6y, F	Skeletal Dysplasia [†]	Basilar – No anomaly Condylar – No anomaly Squama – No anomaly	Ant. arch – No anomaly Post. arch – No anomaly LM – dysplasia Facets -dysplasia	Dens – No anomaly Neural arch – bilateral C2 pars lysis	Dysplasia	V ₃ 1 V ₃ 2 – VA coursing through the lytic defect V ₃ 3 – No anomaly Codominant VA	A
Case 7	7+10y, F	Os odontoideum	Basilar – No anomaly Condylar – No anomaly Squama – No anomaly	No anomalies Facets – No anomaly	Dens – Os Neural arch – No anomaly	No anomaly	V ₃ 1 – No anomaly V ₃ 2 – No anomaly V ₃ 3 – No anomaly Right dominant VA	C
Case 8	6+1y, M	Skeletal Dysplasia [*]	Basilar – No anomaly Condylar – No anomaly Squama – No anomaly	Ant. arch – No anomaly Post. arch – bifid + bulbous ends LM – No anomaly Facets - dysplasia	Dens – Aplasia Neural arch – No anomaly	Dysplasia	V ₃ 1 – HRVA bilateral V ₃ 2 – No anomaly V ₃ 3 – No anomaly Codominant VA	B
Case 9	7+5y, M	Os odontoideum	Basilar – No anomaly Condylar – No anomaly Squama – No anomaly	No anomalies Facets – No anomaly	Dens – Os Neural arch – No anomaly	No anomaly	V ₃ 1 – No anomaly V ₃ 2 – No anomaly V ₃ 3 – No anomaly Codominant VA	C
Case 10	7+3y, F	Os odontoideum	Basilar – No anomaly Condylar – No anomaly Squama – No anomaly	No anomalies Facet – No anomaly	Dens – Os Neural arch – No anomaly	No anomaly	V ₃ 1 – No anomaly V ₃ 2 – No anomaly V ₃ 3 – No anomaly Codominant VA	B
Case 11	2+5y, M	Congenital Anomaly	Basilar – No anomaly Condylar – Hypoplasia Squama – Midline keel off to left	Ant. arch – aplasia Post. arch – bifid + in-curling of edges LM – splayed Facets – No anomaly	Dens – Hypoplasia Neural arch – [R] C2 lamina fused to C3 lamina [L] hemiarch aplasia	C2-C3 lamina fused on [R]	V ₃ 1 – No anomaly V ₃ 2 – No anomaly V ₃ 3 – No anomaly Codominant VA	A
Case 12	3+9y, F	Congenital Anomaly	Basilar – No anomaly Condylar – Hypoplasia Squama – No anomaly	Ant. arch – assimilated Post. arch – assimilated & in-curved in FM LM – assimilated Facets – Vertical oriented	Dens – Hypoplasia Neural arch – C2-3 fusion	No anomaly below C3	V ₃ 1 – No anomaly V ₃ 2 V ₃ 3 – Type 1 bilaterally Codominant VA	A

(continued on next page)

Table 2 (continued)

	Age	Etiology	Occiput	C1	C2	C3-C7	Vertebral Artery (VA)	Grade
Case 13	11+7y, F	Congenital Anomaly [†]	Basilar – No anomaly Condylar – Hypoplasia Squama – No anomaly	Ant. Arch – No anomaly Post. Arch – bifid LM – No anomaly Facets – vertical oriented	Dens – No anomaly Neural arch – C2-3 fusion	No anomaly below C3	V ₃ 1 – HRA bilateral V ₃ 2 – No anomaly V ₃ 3 – [R] PFIA; [L] No anomaly Codominant VA	A
Case 14	6+10y, M	Skeletal Dysplasia*	Basilar – No anomaly Condylar – Hypoplasia Squama – Invaginated opisthion	Ant. arch – bifid Post. arch – bifid LM – not splayed Facets – dysplasia	Dens – Hypoplasia Neural arch – No anomaly	Dysplasia	V ₃ 1 – Bilateral HRVA V ₃ 2 – No anomaly V ₃ 3 – No anomaly Codominant VA	A
Case 15	12+2y, M	Congenital Anomaly [†]	Basilar – Platybasia Condylar – No anomaly Squama – No anomaly	Ant. arch – assimilated Post. arch – assimilated LM – assimilated Facets – vertical oriented	Dens – Hypoplasia Neural arch – C2-3 fusion	Fusions C7-T1 (KFS)	V ₃ 1 – No anomaly V ₃ 2 V ₃ 3 – [R] Type 3 [L] Type 2 Right dominant VA	A
Case 16	2+2y, M	Congenital Anomaly	Basilar – No anomaly Condylar – No anomaly Squama – No anomaly	Ant. arch – bifid Post. arch – bifid LM – splayed Facets – No anomaly	Dens – No anomaly Neural arch – C2-3 fusion	No anomaly below C3	V ₃ 1 – No anomaly V ₃ 2 – No anomaly V ₃ 3 – No anomaly Codominant VA	A
Case 17	6+6y, F	Down Syndrome	Basilar – No anomaly Condylar – No anomaly Squama – No anomaly	No anomalies Facets – No anomaly	Dens – Os Neural arch – No anomaly	No anomaly	V ₃ 1 – No anomaly V ₃ 2 – No anomaly V ₃ 3 – No anomaly Codominant VA	B
Case 18	11y, M	Congenital Anomaly [†]	Basilar – No anomaly Condylar – No anomaly Squama – No anomaly	Ant. arch – assimilated Post. arch – assimilated LM – assimilated Facets – vertical oriented	Dens – No anomaly Neural arch – C2-3 fusion	No anomaly below C3	V ₃ 1 – [L] HRVA [R] no anomaly V ₃ 2, V ₃ 3 – [L] Type 2; [R] Type 3 Right dominant VA	A
Case 19	8+3y, F	Os odontoideum	Basilar – No anomaly Condylar – No anomaly Squama – No anomaly	No anomalies Facets – No anomaly	Dens – Os Neural arch – No anomaly	No anomaly	V ₃ 1 – No anomaly V ₃ 2 – No anomaly V ₃ 3 – No anomaly Left dominant VA	B
Case 20	3+7y, F	Congenital Anomaly	Basilar – No anomaly Condylar – No anomaly Squama – No anomaly	Ant. arch – No anomaly Post. arch – aplasia LM – splayed Facets – No anomaly	Dens – Aplasia Neural arch – C2-3-4 fusion	Fusions C2-3-4 (KFS)	V ₃ 1 – [L] HRVA; [R] no anomaly V ₃ 2 – No anomaly V ₃ 3 – [L] PFIA; [R] No anomaly Left dominant VA	A
Case 21	3+6y, F	Down Syndrome	Basilar – No anomaly Condylar – No anomaly Squama – No anomaly	Ant. arch – synchondrosis unfused Post. arch – bifid & in-curling of edges LM – splayed on [L] Facets – No anomaly	Dens – Hypoplasia Neural arch – No anomaly	No anomaly	V ₃ 1 – No anomaly V ₃ 2 – No anomaly V ₃ 3 – No anomaly Codominant VA	A
Case 22	8+8y, M	Skeletal Dysplasia	Basilar – No anomaly Condylar – Hypoplasia Squama – No anomaly	Ant. arch – bifid Post. arch – bifid LM – No anomaly Facets – No anomaly	Dens – Os Neural arch – No anomaly	No anomaly	V ₃ 1 – [L] HRVA; [R] No anomaly V ₃ 2 – No anomaly V ₃ 3 – No anomaly Codominant VA	A
Case 23	5y, M	Skeletal Dysplasia	Basilar – Hypoplasia Condylar – Hypoplasia Squama – In-curling of opisthion with thickening	Ant. arch – bifid Post. arch – bifid LM – splayed Facets - dysplasia	Dens – Hypoplasia Neural arch – Dysplastic	Dysplasia	V ₃ 1 – No anomaly V ₃ 2 – No anomaly V ₃ 3 – No anomaly Codominant VA	A
Case 24	2+8y, M	Congenital Anomaly	Basilar – No anomaly Condylar – No anomaly Squama – No anomaly	Ant. arch – Synchondrosis unfused Post. arch – No anomalies LM – No anomalies Facets – No anomaly	Dens – Hypoplasia Neural arch – Aplasia	C3 arch hypertrophy	V ₃ 1, V ₃ 2 – No anomaly V ₃ 3 – [R] PFIA; [L] No anomaly Codominant VA	A
Case 25	11y, F	Congenital Anomaly	Basilar – No anomaly Condylar – Hypoplasia Squama – No anomaly	Ant. arch – No anomaly Post. arch – No anomaly LM – No anomaly Facets – Vertical oriented	Dens – Aplasia Neural arch – Bifid	No anomaly	V ₃ 1 – [L] no anomaly; [R] HRVA V ₃ 2 – No anomaly V ₃ 3 – No anomaly Codominant VA	A

VA= Vertebral artery; HRVA = High riding vertebral artery; PFIA = Persistent first intersegmental artery, LM = Lateral mass; KFS= Klippel Feil Syndrome; [R] = right; [L] = left.

* Morquio Syndrome

[†] Basilar invagination # Anomalies in the occipital bone were identified in the basilar, condylar and squamous regions.

Table 3

Planning of screw anchors and the actual surgery performed for patients listed in chronological order (reasons for unsuitability of screws are mentioned in brackets).

	C1LMS	C2PS	C2PaS	TAS	C2LAM	C3LMS	Grade	Surgery Performed	Comment
Case 1	R S L S	S S	S S	US (partial reduction) US (partial reduction)	S* S*	S S	A	C1-C3 fusion , [B/L] C1LMS, [B/L] C2LAM, [B/L] C3LAM	As planned
Case 2	R US (splayed LM) L US (splayed LM)	US (HRVA) US (HRVA)	S S	US (HRVA) US (HRVA)	US (thin lamina) US (thin lamina)	S S	A	O-C3 fusion , [B/L] C2PaS [R]	Not as planned [L] C3LMS cut out intraoperatively
Case 3	R US (inaccessible) L US (inaccessible)	US (HRVA) US (HRVA)	S S	US (HRVA) US (HRVA)	S* S*	S S	A	O-C3 fusion [B/L] C2LAM	As planned
Case 4	R US (inaccessible) L US (inaccessible)	US (HRVA) S	US (too short) S	US (partial reduction) US (partial reduction)	S* S*	S S	A	O-C3 fusion [B/L] C2LAM [B/L] C3LMS	As planned
Case 5	R S L S	S S	S S	S S	S S	S S	A	O-C2 fusion [L] C1LMS [B/L] C2PS	Not as planned VA injury during [R] C1LMS
Case 6	R US (hypoplastic) L US (hypoplastic)	US (pars lysis) US (pars lysis)	US (pars lysis) US (pars lysis)	US (pars lysis) US (pars lysis)	US (pars lysis) US (pars lysis)	US (dysplasia) US (dysplasia)	A	O-C6 fusion [B/L] C5/6 hook [B/L] C5/6 hook	As planned
Case 7	R S L S	S S	S S	US (partial reduction) US (partial reduction)	US (thin lamina) US (thin lamina)	S S	A	O-C2 fusion [B/L] C2PS	As planned
Case 8	R S L S	US (HRVA) US (HRVA)	US (too short) US (too short)	US (HRVA) US (HRVA)	S [^] S [^]	US (dysplasia) US (dysplasia)	A	O-C3 fusion [B/L] C3 hook	Not as planned C2LAM attempted cut out (wrong entry)
Case 9	R S L S	S S	S S	S S	S S	S S	A	C1-C2 fusion [B/L] TAS	As planned
Case 10	R S L S	S US (HRVA)	S S	S S	US (thin lamina) S	S S	A	C1-C2 fusion [B/L] C1LMS [B/L] C2PaS	As planned
Case 11	R US (hypoplastic) L US (hypoplastic)	S US (aplasia)	US (too short) US (aplasia)	US (splayed LM) US (aplasia)	S* S*	US (too small) US (too small)	A	O-C3 fusion [B/L] C2LAM	As planned
Case 12	R US (inaccessible) L US (inaccessible)	S S	S US (too short)	US (partial reduction) US (partial reduction)	S* US* (thin lamina)	S S	A	O-C3 fusion [R] C2LAM, [L] C2PS	As planned
Case 13	R US (inaccessible & VA anomaly) L US (inaccessible)	US (HRVA) S	US (too short) US (too short)	US (partial reduction) US (partial reduction)	US* (thin lamina) S*	S S	A	O-C3 fusion [L] C2PS, [L] C2LAM [R] C3LMS	As planned
Case 14	R S L S	S S	S S	S S	S S	US (dysplasia) US (dysplasia)	A	O-C2 fusion [B/L] C2LAM	As planned
Case 15	R US (inaccessible) L US (inaccessible)	S S	S S	US (partial reduction) US (partial reduction)	S* S*	US (too small) US (too small)	A	O-C3 fusion [B/L] C2PS [B/L] C2LAM	As planned
Case 16	R US (hypoplastic) L US (hypoplastic)	S S	US (too short) US (too short)	S S	US* (thin lamina) US* (thin lamina)	US (too small) US (too small)	A	C1-C2 fusion [B/L] TAS	As planned
Case 17	R S L S	S S	S S	S S	S S	S S	A	C1-C2 fusion [B/L] TAS	As planned
Case 18	R US (inaccessible) L US (inaccessible)	S US (HRVA)	S S	US (partial reduction) US (partial reduction)	S* S*	US (too small) US (too small)	A	O-C3 fusion [B/L] C2LAM	As planned
Case 19	R S L S	S S	S S	S S	S S	S S	A	C1-C2 fusion [B/L] TAS	As planned
Case 20	R US (VA anomaly & splayed LM) L US (inaccessible & splayed LM)	S US (HRVA)	US (too short) US (too short)	US (splayed LM) US (splayed LM, HRVA)	S* S*	S S	A	O-C2 fusion [R] C2PS, [L] C2LAM	As planned
Case 21	R S L S	S S	S S	S S	US (thin lamina) US (thin lamina)	US (too small) US (too small)	A	C1-C2 fusion [B/L] TAS	As planned
Case 22	R S L S	S US (HRVA)	S S	US (no trajectory) US (HRVA)	S [^] S [^]	US (dysplasia) US (dysplasia)	A	O-C2 fusion [L]C2LAM, [R] C2PS	As planned
Case 23	R US (hypoplastic & splayed LM) L US (hypoplastic & splayed LM)	US (hypoplasia) US (hypoplasia)	US (too short) US (too short)	US (splayed LM) US (splayed LM)	S [^] S [^]	US US	A	O-C2 fusion Sublaminar Mersilene tapes	Not as planned All attempted laminar screws cut out intraop
Case 24	R US (hypoplastic, VA anomaly) L US (hypoplastic)	US (aplasia) US (aplasia)	US (aplasia) US (aplasia)	US (aplasia) US (aplasia)	US (aplasia) US (aplasia)	US (too small) US (too small)	A	O-C3 fusion [L] C3PS [R] C3LAM	As planned
Case 25	R US (hypoplastic) L US (hypoplastic)	US (HRVA) S	US (too short) S	US (partial reduction) US (partial reduction)	S [^] S [^]	US (too small) US (too small)	A	O-C2 fusion [B/L] C2LAM	As planned

S = Suitable; US = Unsuitable; VA = vertebral artery; HRVA = high riding vertebral artery; C1LMS = C1 lateral mass screw; C2PS = C2 pedicle screw; C2PaS = C2 pars screw; TAS = Transarticular screw; C2LAM = C2 laminar screw; C3LMS = C3 lateral mass screw; R = right; L = left; B/L = bilateral; LM = Lateral mass.

[^] Uncrossed screw trajectory for C2LAM screws

* C2-3 congenital fusion

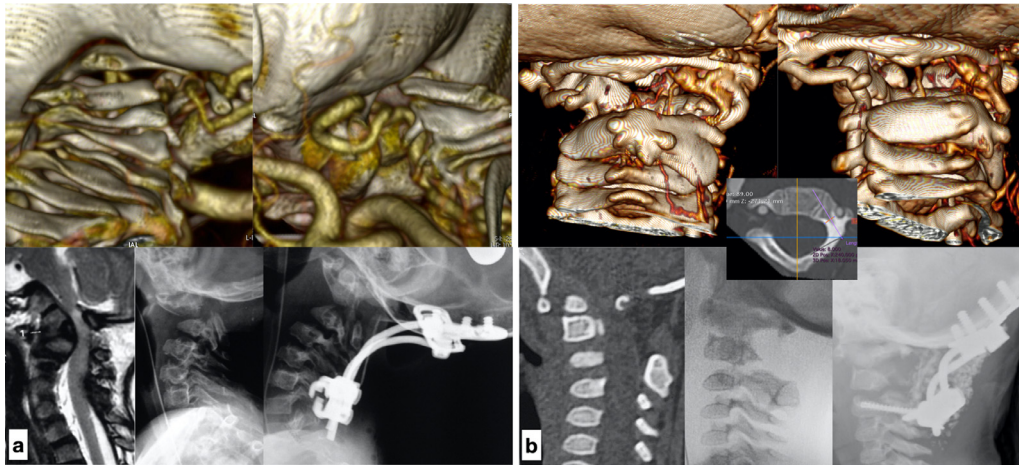


Fig. 4. Two cases where C2 screws anchors were not possible. (a) Bilateral C2 pars lysis - Case 6 and (b) Congenital aplasia of C2 neural arch - Case 24.

Table 4

Table summarising the causes of unsuitability of screws in C1 and C2.

	Suitable sites	Unsuitable sites	Causes of Unsuitability	Planned	Successfully inserted
C1LMS	22	28	Hypoplasia (n = 12) Splayed LM (n = 6) Inaccessible (n = 13) VA anomaly (n = 3)	8	5 (62.5%)
C2PS	30	20	HVRA (n = 13) Aplasia of neural arch (n = 3) Hypoplasia (n = 2) C2 pars lysis (n = 2)	10	10 (100%)
TAS	16	34	Partial reduction (n = 16) Splayed LM (n = 5) HRVA (n = 8) Pars lysis (n = 2) Aplasia of neural arch (n = 3)	10	10 (100%)
C2LAM	35	15	Thin lamina (n = 11) Aplasia (n = 2) Pars lysis (n = 2)	24	20 (83%)
C2PaS	31	19	Too short (n = 14) C2 pars lysis (n = 2) Aplasia neural arch (n = 3)	4	4 (100%)

C1LMS = C1 lateral mass screw; C2PS = C2 pedicle screw; TAS = transarticular screw; C2LAM = C2 laminar screw; C2PaS = C2 pars screw; LM = lateral mass; VA = Vertebral artery.

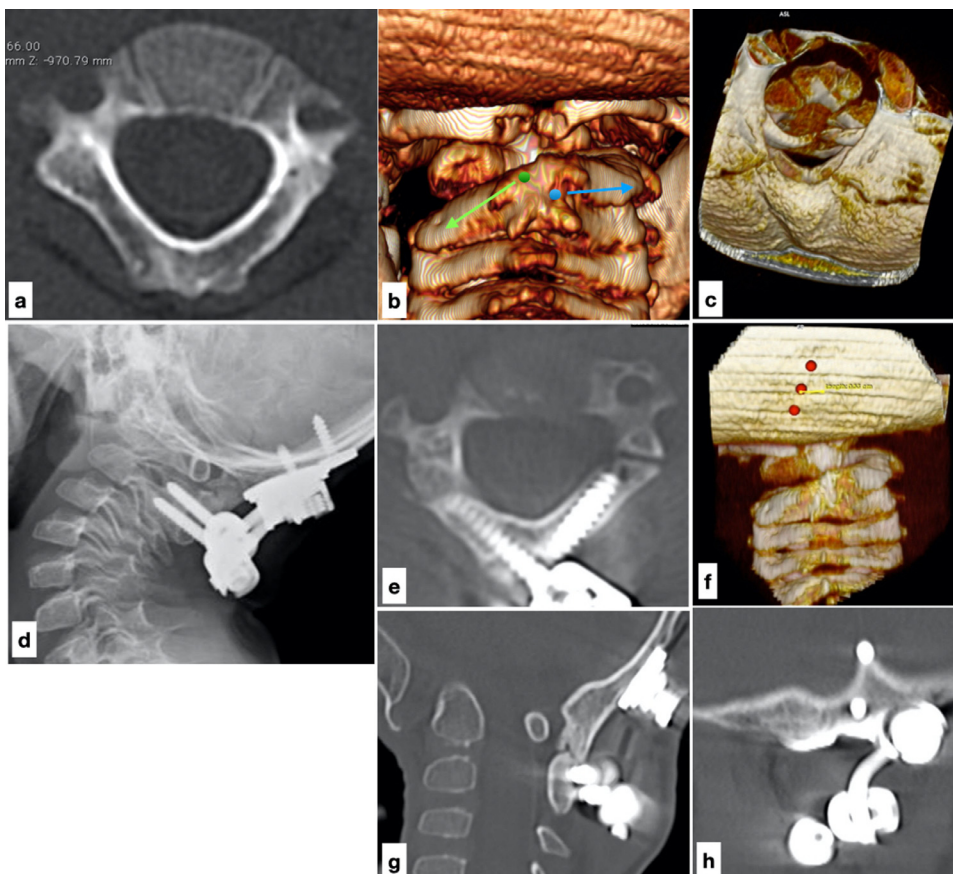


Fig. 5. Case 11: Note the altered entry points of the C2 laminar screws if an in-line trajectory is planned (a). These entry points are ipsilateral to the side to the lamina to be instrumented and have an uncrossed pattern (b, e). The 3D reconstruction shows the midline keel off to the left side (c, f). Postoperative CT scan shows regeneration of the excised C1 posterior arch (g).

15–1300 ml), and the average surgical time was 185 min (range 150–300).

Neurological outcomes and fusion

The clinico-radiological outcomes are summarized in Table 1. The mean follow-up was 25 months (range 6–48 months). Neurology improved in all except one patient who had a neurological deterioration. Average postoperative UE and LE mJOA scores were 4.3 (range 0–5) and 5.8 (range 1–7).

Postoperative CT scan showed partial loss of reduction in three patients without spinal cord compromise (12%). Fusion was achieved in all patients. In one patient, the excised C1 posterior arch reformed without any neurological compression. Out of the 24 screws passed through the C2 pars (C2PS, TAS, and C2PaS), three (12.5%) screws violated the vertebral artery cave without any adverse effect. There were no malpositions detected in the other screw types.

Complications

Three patients (12%) had complications in this series. One patient (Case 5) had a VA injury while exposing to the C1LMS. Two patients underwent revision surgery.

A 5-year old with Morquio syndrome (Case 8), with preoperative mJOA UE and LE of 1 and 2, respectively with syringomyelia and syringobulbia with cervical cord signal changes underwent an emergent revision surgery as he developed a postoperative neurological worsening (mJOA 0 and 1 in UE and LE, respectively) due to hook migration into the spinal canal. There was no improvement after surgery, and the child underwent a tracheostomy and was ventilator-dependent at the last follow-up of 1 year.

The second revision surgery was in an 11+7year old girl with congenital basilar invagination, who had a C3LMS failure detected 7 days after surgery (Case 13). This screw was removed, and the fixation was augmented with Mersilene tapes. The patient completely recovered neurologically but did have a partial loss of radiographic correction.

Discussion

Several authors have recommended that a multiplanar reconstruction of CT images is necessary to plan screw trajectories in the C2 vertebra, as standard orthogonal CT slices are not in the plane of the screw path [5–8]. Since many hospital PACS do not have radiology workstation capabilities to perform multiplanar reconstructions; such planning invariably has to be done in the radiology department [15].

Some hospitals have PACS that allows the end-user to perform MPR. The four steps described in this paper can be used on any software with MPR capabilities. However, if the hospital PACS does not have MPR functionality, then invariably preoperative planning requires the surgeon to take help of the radiology department.

This above-noted method has several shortcomings. Foremost, the surgeon can only spend limited time on preoperative planning in the radiology department. Once the desired images are reconstructed with the radiologist's help and exported to PACS, they cannot be re-manipulated later without a repeat visit to the radiology department. Moreover, we believe the most crucial disadvantage is the surgeon's inability to manipulate the images personally. A radiologist manipulating the DICOM images is akin to the surgeon observing an anatomy dissection rather than doing it.

We believe that the surgeon gains far greater anatomical knowledge by manipulating the DICOM images on his laptop, rather than depending on a radiologist. The 3D volume rendering of the pathoanatomy is available to the surgeon in the operating room on the laptop.

We found substantial new information using Horos™ (Grade A) regarding screw trajectory planning in all patients compared to PACS. This

is not surprising as many authors have proposed MPR CT for preoperative planning of these screws [5,6,8]. In this series, the most common screw anchor in the C2 was the C2LAM. Considering the safety profile of this screw, we have found this screw to be an excellent alternative to the C2PS, especially in patients with congenital C2-3 fusions. However, we found that not all laminae were thick enough for instrumentation despite C2-3 fusion, and we found 30% of sites (15 out of 50 sites) unsuitable. Even in patients with congenital C2-3 fusion, 20% sites were unsuitable for C2 laminar screws. Hence preoperative assessment of lamina thickness in the line of the screw trajectory becomes essential to avoid screw cut out.

We found that very young (<5-year-olds) and skeletal dysplasia children had an underdeveloped C2 spinous process necessitating an unconventional entry point with an uncrossed trajectory for the C2LAM (Fig. 5). An in-line trajectory of the C2 lamina pointed the entry on the ipsilateral side of the C2 spinous process rather than its contralateral base. Using such entry points, the screws were placed in an uncrossed pattern (Video supplement 2), in-line with the laminar axis rather than the typical crossed screws described in the literature [16]. Scuibba et al. used such an uncrossed trajectory using ipsilateral entry point in 2 out of 16 adult patients (12.5%) due to the presence of a bifid C2 lamina [17]. In pediatric patients, it seems that a much higher percentage of patients (28%) require an ipsilateral uncrossed trajectory as shown in our series. An alternative to this in-line and intraosseous trajectory is the technique used by Savage et al. in their series of less than 5-year-olds where the authors have used a modified Wright technique with an intentional exit point on the contralateral side [18].

Concerning local pathoanatomy, we found that 3D volume rendering on Horos™ provided substantial new information (Grade A) in 72% of patients compared to PACS. The main differentiating feature of 3D reconstructions on Horos™ is the surgeon's ability to visualize the 3D image in any projection after cropping out unwanted areas. This is in contrast to the 3D images provided on PACS, which are created by radiology technicians. Not only are these images frequently not as per the surgeon's viewpoint, but also, they cannot be manipulated in three dimensions. A clear understanding of deformed anatomy can boost the surgeon's confidence as the surgical exposure is executed with conviction (Figs. 4,5). An exploratory approach during surgery could injure vital structures, especially if the abnormal anatomy is unanticipated.

In 4 (16%) patients, at least one screw in the construct could not be executed as planned on Horos™. We found particular problems with C3LMS and C2LAM. In two patients, C3LMS cut out once intraoperatively and in another in the acute postoperative period. Because C3LMS were supplementary to C2 screw anchors, the fixation could be salvaged in both patients. C2LAM screw problems were encountered in two dysplasia patients who had an intraoperative cut out of the screw, despite of preoperative planning suggesting adequate lamina width. These situations illustrate the problems faced in pediatric CVJ surgery, especially while instrumenting small, soft dysplastic bones.

Alternative fixation methods such as Mersilene® tapes should be kept handy if the main fixation in C2 fails. Mersilene® tapes have a broader foot print that distributes the load over a wider area compared to wires and cable that, in our experience, tend to cut out of soft pediatric bone. Hooks can be used as salvage fixation in relatively older children. However, we will caution the use of hooks in the very young with small posterior elements, especially those with soft dysplastic bones, as we have experienced a serious complication of hook migration in one patient.

Complications were encountered in 3 patients (12%). This rate seems comparable to that reported in a meta-analysis that found a complication rate of 14 and 15% in occipitocervical and atlantoaxial fusion, respectively [1]. However, it is difficult to compare these rates between studies due to a wide variation in reported CVJ pathologies and the ages at which surgeries are done. We feel that our cohort is relatively younger (<12 years) compared with published studies that have included older patients (<18 years) [1]. Moreover, our cohort consists of a higher per-

centage (72%) of congenital anomalies or dysplasia patients than existing literature [1]. And finally, in contrast to our study, previously reported series have included children with normal neurology [19]. Despite these differences, we acknowledge that it is difficult to conclude with our study that this preoperative planning method using Horos™ helps reduce complications.

There are other technologies besides Horos™ that can be useful. 3D printed real-size biomodels can provide three-dimensional anatomical information similar to the 3D volume-rendered images generated by Horos™; however, they are an additional expense [20]. Computer navigation is another technology that can help place challenging pedicle screws, but this is not common place in many countries due to cost limitations [21]. However, we believe preoperative MPR planning is advisable even if intraoperative computer navigation or 3D printed biomodels are used. The images generated on Horos™ are similar to those generated on the O-arm guided computer navigation console when a particular screw trajectory is chosen [22].

Knowledge of the steps involved in MPR for CVJ, either performed on Horos™ or the computer navigation console before the surgery can help the surgeon plan better and avoid intraoperative surprises. Two decades ago, Newton et al., in their paper, demonstrated the utility of 3D MPR for congenital scoliosis using similar subjective assessments used in this paper. They stated that the limitation of 3D MPR was the necessity of expensive software and trained CT technicians to create reconstructions [14]. With user-friendly open-source software such as Horos™, this is no longer a limitation.

There are some limitations to the current study. Besides being a small series with the experience of two surgeons, it is not easy to objectively prove the benefits of a software like Horos™. A controlled study with a cohort of patients operated prior to the use of Horos™ might give some answers, however, we do not have such a cohort to compare. We chose to use a subjective grading system reported by the operating surgeon in an attempt to objectify the usefulness of MPR. There is a possibility of bias, in that the operating surgeon may have overestimated MPR's usefulness. But we feel that an independent grading by a surgeon not involved in the surgery of the patient will also not be appropriate. This is because, we believe that the benefit derived from such preoperative planning is related to both the complexity of the case and the surgeon's experience. Less experienced surgeons might find this method of preoperative planning useful even for simpler anomalies. However, even the most skilled surgeons may derive benefit from planning on Horos™ in rare and complex cases. We feel, it is difficult to factor in surgeon's capability and case complexity when determining the usefulness of this method of preoperative planning.

Another limitation of the study is the relatively short follow up in pediatric patients. However, the goal of this paper was not to present long term outcomes but to explore the utility of preoperative planning and compare it with intraoperative difficulties and immediate postoperative complications. Finally, because Horos™ is not FDA approved, its adoption will be a significant hurdle in some countries. In a hospital where such barriers exist, the surgeon can still apply these four steps of MPR on FDA-approved radiology workstations. We think that when surgeons personally go through the steps of MPR, they stand to gain more information than from similar MPR done by the radiologist who has limited knowledge of screw trajectories.

Conclusion

In our experience, surgeon-directed DICOM manipulation gives more anatomical information compared to studying PACS images and should be incorporated in the surgeon's preoperative workup. Such planning can be performed on an open-source software like Horos™ or on any other hospital PACS software with MPR functionality. We have described a four-step method supplemented with a video demonstration on how to use MPR for planning screw trajectories for C2 pedicle screw, transarticular screw and C2 laminar screws.

Video 1: Video describing the four steps involved in preoperative planning for C2 laminar screws, C2 pedicle screw and Transarticular screws.

Financial disclosure

None

There was no financial support for this study.

Declarations of Competing Interest

None of the authors have any conflict of interests or financial disclosures.

Supplementary materials

Supplementary material associated with this article can be found, in the online version, at [doi:10.1016/j.nxj.2021.100073](https://doi.org/10.1016/j.nxj.2021.100073).

References

- [1] Hwang SW, Gressot LV, Rangel-Castilla L, et al. Outcomes of instrumented fusion in the pediatric cervical spine: clinical article. *J Neurosurg Spine* 2012;17(5):397–409.
- [2] Zhang YH, Zhou FC, Zhang J, et al. Efficacy and safety of atlantoaxial fluoroscopy-guided pedicle screw fixation in patients younger than 12 Years: a radiographic and clinical assessment. *Spine* 2019;44(20):1412–17.
- [3] Janjua MB, Hwang SW, Samdani AF, et al. Instrumented arthrodesis for non-traumatic craniocervical instability in very young children. *Child's Nerv Syst* 2019;35(1):97–106.
- [4] Gluf WM, Schmidt MH, Apfelbaum RI. Atlantoaxial transarticular screw fixation: a review of surgical indications, fusion rate, complications, and lessons learned in 191 adult patients. *J Neurosurg Spine* 2005;2(2):155–63.
- [5] Brockmeyer DL, York JE, Apfelbaum RI. The anatomical suitability of C1-2 transarticular screw placement in pediatric patients. *Neurosurg Focus* 1999;6(6):8.
- [6] Ould-Slimane M, Pape SL, Leroux J, et al. CT analysis of C2 pedicles morphology and considerations of useful parameters for screwing. *Surg Radiol Anat* 2014;36(6):537–42.
- [7] Marques LMS, d'Almeida GN, Cabral J. Two-step™ technique with OsiriX™ to evaluate feasibility of C2 pedicle for surgical fixation. *J Craniovertebr Junction Spine* 2016;7(2):75–81.
- [8] Resnick DK, Lapsiwala S, Trost GR. Anatomic suitability of the C1-C2 complex for pedicle screw fixation. *Spine* 2002;27(14):1494–8.
- [9] Davidson C, Bergin P, Varney E, et al. Planning C2 pedicle screw placement with multiplanar reformatted cervical spine computed tomography. *J Craniovertebr Junction Spine* 2019;10(1):46.
- [10] Benzel EC, Lancon J, Kesterson L, et al. Cervical laminectomy and dentate ligament section for cervical spondylotic myelopathy. *J Spinal Disord* 1991;4(3):286–95.
- [11] Cacciola F, Phalke U, Goel A. Vertebral artery in relationship to C1-C2 vertebrae: an anatomical study. *Neurol India* 2004;52(2):178–84 PMID: 15269464.
- [12] Wang S, Wang C, Liu Y, et al. Anomalous vertebral artery in craniocervical junction with occipitalization of the atlas. *Spine* 2009;34(26):2838–42.
- [13] Yamazaki M, Koda M, Aramomi M, et al. Anomalous vertebral artery at the extraosseous and intraosseous regions of the craniocervical junction: analysis by three-dimensional computed tomography angiography. *Spine* 2005;30(21):2452–7.
- [14] Newton PO, Hahn GW, Fricka KB, et al. Utility of three-dimensional and multiplanar reformatted computed tomography for evaluation of pediatric congenital spine abnormalities. *Spine* 2002;27(8):844–50.
- [15] Vizurraga DE, Rhee JM, Borden TC, et al. Inline™ axial reconstructed CT scans provide a significantly larger assessment of C2 pedicle diameter for screw placement compared with "standard" axial scans: implications for surgical planning. *Clin Spine Surg* 2017;30(8):E1039–45.
- [16] Wright NM. Posterior C2 fixation using bilateral, crossing C2 laminar screws: case series and technical note. *J Spinal Disord* 2004;17(2):158–62.
- [17] Sciubba DM, et al. Laminar screw fixation of the axis. *J Neurosurg Spine* 2008;8:327–34.
- [18] Savage JG, Fulkerson DH, Sen AN, et al. Fixation with C-2 laminar screws in occipitocervical or C1-2 constructs in children 5 years of age or younger: a series of 18 patients: clinical article. *J Neurosurg Pediatr* 2014;14:87–93.
- [19] Helenius IJ, Bauer JM, Verhofsfe B, et al. Os Odontoideum in children: treatment outcomes and neurological risk factors. *J Bone Jt Surg* 2019;101(19):1750–60.
- [20] Goel A, Jankharia B, Shah A, et al. Three-dimensional models: an emerging investigational revolution for craniocervical junction surgery. *J Neurosurg Spine* 2016;25(6):740–4.
- [21] Rajasekaran S, Kanna RM, Shetty AP. Intra-operative computer navigation guided cervical pedicle screw insertion in thirty-three complex cervical spine deformities. *J Craniovertebr Junction Spine* 2010;1(1):38.
- [22] Yin D, Oh G, Neckrysh S. Axial and oblique C2 pedicle diameters and feasibility of C2 pedicle screw placement: technical note. *Surg Neurol Int* 2018;9(1):40.